JOURNAL OF SPACECRAFT AND ROCKETS
Vol. 35, No. 6, November–December 1998

Real-Time Optimal Attitude Estimation Using Horizon Sensor and Magnetometer Data

Steven M. Hill* and Todd J. McCusker†
Space Industries, Inc., League City, Texas 77573

Full three-axis knowledge was desired for a momentum bias spacecraft employing only a horizon sensor for attitude determination. This sensor provided adequate knowledge for rotations about two axes but no information for rotations about the nadir axis. Though satisfactory for many applications, proximity and rendezvous operations of a thrusting vehicle near the Shuttle are best supported with three-axis knowledge. The solution devised takes three-axis magnetometer outputs, used on the spacecraft to scale magnetic torquer commands, and horizon sensor outputs to establish an overdetermined attitude matrix. The attitude matrix is solved by minimizing a chi-square loss function relating the measured vectors to internally modeled reference vectors. The reference vectors are provided by a Keplarian propagator modified for oblateness effects and the 1995 World Magnetic Model 12th-order geomagnetic field coefficients. The approach is implemented on a laptop computer for real-time flight operations. Ground simulations indicate three-sigma errors of about 1.3 deg in pitch and roll and 2.6 deg in yaw. Tests conducted on the Shuttle's robot arm prior to release of the spacecraft on STS-69 and STS-80 confirmed these expectations. The system performed well during free flight and provided valuable attitude knowledge during perturbations due to tip-off and thruster alignment uncertainties.

Nomenclature

$\boldsymbol{A}$	= attitude matrix (3×3) relating body orientation to local vertical–local horizontal orientation
$\boldsymbol{B}$	= geomagnetic field vector, nT
G	= sequential filter gain
g, h	= spherical harmonic coefficients, nT
I_θ	= pitch torquer command, mA
J	= loss function, equivalent to χ^2
J'	= modified loss function
J_2	= largest zonal coefficient in spherical harmonic expansion of Earth's gravitational potential
$k_{1,2}$	= pitch torquer position gains, mA/nT-rad
k_3	= pitch torquer rate gain, mA-s/nT-rad
$\hat{\boldsymbol{n}}$	= unit nadir vector
P	= Legendre polynomial
$\boldsymbol{q}$	= attitude quaternion
$\boldsymbol{r}$	= spacecraft position vector, m
r_e	= equatorial radius of Earth, m
$\hat{\boldsymbol{u}}$	= unit attitude vector
V	= geomagnetic scalar potential, nT-m
$\boldsymbol{V}$	= weighted reference vector
$\boldsymbol{W}$	= weighted measurement vector
w	= weighting factors
x, y, z	= coordinate axes in an orthogonal right-handed system
α	= orthogonality metric
β	= B-field error angle, rad
Θ	= colatitude, rad
θ	= pitch angle, rad
λ	= eigenvalue
σ	= uncertainty (1 standard deviation) in a parameter
Φ	= longitude, rad
ϕ	= roll angle, rad
ψ	= yaw angle, rad
ω	= instantaneous body rate, rad/s

Received Jan. 12, 1998; revision received July 14, 1998; accepted for publication July 16, 1998.

*Project Engineer; currently Graduate Research Assistant, Laboratory for Atmospheric and Space Physics, University of Colorado, Campus Box 392, Boulder, CO 80309-0392. Member AIAA.

†Project Engineer; currently Senior Systems Engineer, Systems Engineering Department, Lockheed Martin Missiles and Space, Org. EA-3D, 4820 E. Dry Creek Road, Littleton, CO 80122-3701.

Introduction

THE development of an operational tool to maximize knowledge of a Shuttle free flyer's attitude state given limited telemetry and onboard processing is described. The Wake Shield Facility (WSF) has flown three times since 1994. The spacecraft must maintain pointing accuracy of ± 10 deg about its velocity vector to support its primary science mission, which is to grow thin film gallium–arsenide wafers using ultravacuum techniques.[1] The fairly loose pointing accuracy is more than sufficient to guarantee a proper ultravacuum wake behind the free flyer as it operates in a ~200-n mile circular orbit, after being released by the Space Shuttle.

The WSF attitude determination and control system (ADACS) is a magnetically dumped momentum bias system[2] requiring only pitch and roll information and the geomagnetic field vector (referred to as the B-field) in body coordinates. The substantial momentum bias about the pitch axis is provided by a constant-speed momentum wheel and a variable-speed reaction wheel, which also provides pitch control. Roll and pitch are measured with a spinning horizon sensor incorporated into the momentum wheel, whereas yaw (rotation about the orbit radius vector) is not sensed onboard at all. A single magnetic torquer aligned with the pitch axis is used to control roll, and quarter-orbit coupling is used to indirectly control yaw. The ADACS also utilizes yaw and roll magnetic torquers for reaction wheel momentum management and a three-axis fluxgate magnetometer for B-field sensing.

A drawback of a system of this type is that information about yaw is not directly available; thus, it is difficult to verify that the proper pointing tolerances are met. Furthermore, because of the WSF's extreme sensitivity to contamination, the Shuttle cannot fire its thrusters to separate from the free flyer. The WSF achieves the desired separation by firing a 2-oz cold nitrogen thruster for approximately 20 min. During the critical thrusting period, concerns naturally arise over the accuracy of the trajectory the WSF follows when departing from the Shuttle. Thus, real-time knowledge of the yaw performance is highly desirable.

The solution implemented for WSF-02 and WSF-03 missions, which flew on Shuttle flights STS-69 and STS-80, was a ground-based, real-time attitude estimation program for flight controllers. The algorithm combines magnetometer data and horizon sensor data to compute an optimal single-frame attitude estimate. In addition, the program produces the following previously unavailable parameters: filtered angular rates, a comparison of the expected B-field body vector to that observed, manual pitch torquer command levels, and a metric of overall accuracy. The system has demonstrated excellent performance on both missions. This paper presents a summary of the approach and implementation along with test and flight operations results from the STS-69 and STS-80 missions.

Mathematical Model

This section describes the mathematical model, including relevant coordinate systems, used to establish the B-field and nadir vectors for the desired attitude of the spacecraft. These desired vectors are then compared to the actual spacecraft measurements and used to compute an optimal three-axis attitude estimate. Additional features, such as rate filtering, are then discussed.

Coordinate Systems

A key first point is to describe the five coordinate systems used in the model: M50, perifocal, geocentric rotating, local vertical–local horizontal (LVLH), and spacecraft body. All orbit propagation is referenced to M50 (mean equator and equinox of 1950) coordinates. This system is similar to a geocentric inertial system but is tied to the constants of 1950. It is used by the Shuttle flight control team at NASA Johnson Space Center (JSC). Perifocal or orbit plane coordinates is an intermediate system used in the Keplarian orbit propagation. Geocentric rotating coordinates represent the spacecraft position in terms of a system rotating with the Earth at the equinox and equator of date. The LVLH system is a set of local orbital coordinates and is used as the reference for the nominal attitude. The relation between LVLH and spacecraft body coordinates is shown in Fig. 1. The Euler angle rotation sequence is 3–1–2 (yaw–roll–pitch). In the nominal spacecraft attitude, the body and LVLH axes are coincident.

Nadir Vector

The first vector used in the complete attitude solution is the nadir vector of the spacecraft. This vector is observed in body coordinates using pitch and roll measurements from the horizon sensor. The reference nadir vector, in the direction of the negative position vector, is provided by an orbit propagator. "Propagation" is used here to indicate solution of high-level analytic relations as opposed to numerical integration of the equations of motion. Thus, propagation is quicker and more appropriate to a real-time application.

Orbital parameters are provided to the program periodically by the user as instantaneous state vector $\boldsymbol{r}$ and $\dot{\boldsymbol{r}}$ for a given epoch. These are then converted to Keplerian elements using the classical relations.[3] Kepler's equation is solved for the time elapsed since the epoch of the state vector, giving a new true anomaly.[4] The current position of the spacecraft is, thus, determined in perifocal coordinates. To account for oblateness effects, the orbit plane is rotated about Earth's axis according to the J_2 term for nodal regression. Using this newly calculated right ascension of ascending node, the perifocal location of the spacecraft is transformed back to geocentric inertial coordinates. Accommodations are made for the precession and nutation of Earth's axis from 1950 to the epoch of interest.[4] This is necessary to relate the spacecraft position in geocentric inertial coordinates to its position in a geocentric rotating frame. Finally, the negative position vector is normalized and transformed to the LVLH system for use in the attitude estimation kernel. In the LVLH system the nadir vector is always $(0, 0, -1)$, and so this provided a good check of coordinate transformation routines.

As part of the software validation, a comparison was made between the described propagator and a commercial orbit analysis program integrating the equations of motion. The commercial program included a comprehensive set of perturbing forces, and its results were taken to be truth. The spacecraft positions were within 60 n miles of each other 12 h after the initial state vector epoch. Because the WSF was to fly 40 ± 25 n miles from the Shuttle, 12 h was deemed the maximum time allowed between updating state vectors (provided by the Shuttle flight control team).

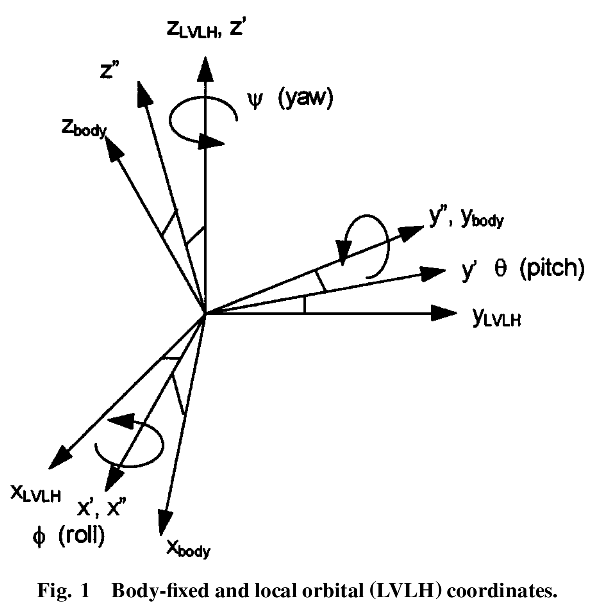

Fig. 1 Body-fixed and local orbital (LVLH) coordinates.

B-Field Vector

The second independent spacecraft attitude vector is provided by Earth's magnetic field. The measurement is made by a three-axis fluxgate magnetometer on the spacecraft. A reference vector is provided by modeling the main field as a spherical harmonic expansion, with spacecraft position provided by the orbit propagator. Short-term variations and small contributions due to ionospheric and magnetospheric electric currents are ignored. Detailed discussion of the application of spherical harmonics to the problem of the geomagnetic field can be found in Refs. 5 and 6. The geomagnetic field satisfies Laplace's equation such that the magnetic field is represented by the gradient of a scalar potential, $\boldsymbol{B} = -\nabla V$. The solution of interest is the outer solution to Laplace's equation in spherical coordinates:

$$V(r, \Theta, \Phi) = r_e \sum_{n=1}^{k} \left(\frac{r_e}{r}\right)^{n+1} \sum_{m=0}^{n} (g_{n,m} \cos m\Phi + h_{n,m} \sin m\Phi) \times P_{n,m}(\Theta) \tag{1}$$

where n and m indicate the degree and order of the terms. The convention used for field direction is that the field has positive value along a vector departing the north-pointing end of a typical dipole bar magnet. Care is taken to properly normalize the coefficients $g_{n,m}$ and $h_{n,m}$, and a recursion formula is used to compute the Legendre polynomials $P_{n,m}$. The gradient taken in spherical coordinates gives the magnetic field vector in geocentric spherical (rotating) coordinates. The vector is then converted to LVLH coordinates for comparison to the measured vector.

The coefficients used for flight operations are those of the World Magnetic Model 1995 (Ref. 7) (WMM95). Along with the coefficients are secular terms that allow model accuracy to be maintained over a period of several years.

Combining Attitude Vectors

To completely determine the attitude of a spacecraft, a minimum of three parameters are needed: one due to each rotational degree of freedom. Though a single pointing vector provides three parameters, only two parameters (angles) are independent because there is still a degree of rotational freedom about the vector itself. Either three angles, e.g., Euler angles, or a vector (effectively two angles) and a phase angle are required. If $n > 1$ independent pointing vectors are available, then $2n$ angles are provided, resulting in an overdetermined system. However, it is fairly straightforward to combine vector measurements in an optimal way to arrive at a best estimate of the three determining angles. Recent work and additional references on techniques for solving the overdetermined attitude problem may be found in Ref. 8.

This section briefly outlines the $\boldsymbol{q}$-method approach described by Lerner[9] and initially developed by Wahba.[10] For WSF $n = 2$, the $\boldsymbol{q}$-method is completely general because it is independent of measurement methods and number of pointing vectors. Thus, it has applications for all varieties of attitude determination techniques. The approach is to minimize a chi-square loss function in the form

$$J(\boldsymbol{A}) = \sum_{i=1}^{n} w_i |\hat{\boldsymbol{u}}_{\text{meas},i} - \boldsymbol{A}\hat{\boldsymbol{u}}_{\text{ref},i}|^2 \tag{2}$$

where $w_i = 1/\sigma_i^2$ and $n \geq 2$. The measured vector is in the body frame, and the reference vector is in the LVLH frame. The loss function may be written in modified form as

$$J'(\boldsymbol{A}) = \sum_{i=1}^{n} \boldsymbol{W}_i \boldsymbol{A} \boldsymbol{V}_i \equiv \text{tr}(\boldsymbol{W}^T \boldsymbol{A} \boldsymbol{V}) \tag{3}$$

such that $J \sim -2J' +$ constants and where $\boldsymbol{W}_i = \sqrt{(w_i)}\hat{\boldsymbol{u}}_{\text{meas},i}$ and $\boldsymbol{V}_i = \sqrt{(w_i)}\hat{\boldsymbol{u}}_{\text{ref},i}$. It is clear that maximizing J' is equivalent to minimizing J. If the attitude matrix is parameterized in terms of the quaternion $\boldsymbol{q}$, then

$$J'(\boldsymbol{q}) = \boldsymbol{q}^T \boldsymbol{K} \boldsymbol{q} \tag{4}$$

The (4×4) $\boldsymbol{K}$ matrix is defined as

$$\boldsymbol{K} = \begin{bmatrix} \boldsymbol{S} - 1\gamma & \boldsymbol{Z} \\ \boldsymbol{Z}^T & \gamma \end{bmatrix} \tag{5}$$

where the intermediate matrices $\boldsymbol{B}$ and $\boldsymbol{K}$, vector $\boldsymbol{Z}$, and scalar γ are

$$\boldsymbol{B} \equiv \boldsymbol{W}\boldsymbol{V}^T, \qquad \boldsymbol{S} \equiv \boldsymbol{B}^T + \boldsymbol{B}$$
$$\boldsymbol{Z} \equiv [B_{12} - B_{32}, B_{31} - B_{13}, B_{12} - B_{21}]^T, \qquad \gamma \equiv \text{tr}(\boldsymbol{B}) \tag{6}$$

Once the $\boldsymbol{K}$ matrix is constructed, the remaining problem is an eigenvalue one:

$$\boldsymbol{K}\boldsymbol{q} = \lambda \boldsymbol{q} \tag{7}$$

This eigenvalue equation is solved by means of Jacobi transformations. The solution is composed of four eigenvalues and four eigenvectors. The eigenvector corresponding to the maximum eigenvalue is the best-estimate attitude quaternion. The quaternion is then transformed into the attitude matrix and Euler angles.[11]

Body Rates, Filters, and Other Features

The attitude solution for the free flyer can be processed to yield other data that are operationally useful. The attitude estimation software computes filtered body rates, a B-field error angle, an orthogonality angle that serves as an accuracy estimate, and a value for a manual pitch torquer command for nutation damping and precession control.

Given that a full attitude solution in Euler angle form was produced by the attitude synthesis software, obtaining body rates was merely a matter of differentiating the angle data, filtering appropriately to reduce noise, and transforming it into body coordinates. The raw Euler rates were computed by finite differencing of the Euler angles. These Euler rates were then transformed into body rates and smoothed using a weighted sequential filtering scheme:

$$\omega_{x,i} = \frac{-\dot{\psi}\sin\phi\cos\theta + \dot{\phi}\cos\phi + G\omega_{x,i-1}}{1+G}$$
$$\omega_{y,i} = \frac{\dot{\psi}\sin\theta - \dot{\phi}\cos\theta\sin\phi + \dot{\theta} + G\omega_{y,i-1}}{1+G} \tag{8}$$
$$\omega_{z,i} = \frac{\dot{\psi}\cos\phi\cos\theta + \dot{\phi}\sin\theta\sin\phi + G\omega_{z,i-1}}{1+G}$$

where the index i indicates the current value and $i-1$ indicates the value from the preceding sample.

In the event of loss of horizon sensor data, the magnetometers can still yield useful information on the spacecraft attitude. The angle between the expected B-field and measured value is

$$\beta = \arccos\frac{\boldsymbol{B}_{\text{ref}} \cdot \boldsymbol{B}_{\text{meas}}}{|\boldsymbol{B}_{\text{ref}}||\boldsymbol{B}_{\text{meas}}|} \tag{9}$$

The angle β can be used to establish whether the spacecraft attitude is controlled or significantly perturbed. These data would be useful in trouble shooting an ADACS malfunction.

The accuracy of the attitude solution is directly dependent on the angle between the reference B-field and reference nadir vectors. Accuracy is at a maximum when they are orthogonal. As they approach being parallel, the solution decreases in accuracy. Because the B-field is not constant throughout the orbit, the accuracy varies. The angle between the vectors is used as a qualitative indicator of accuracy during flight operations:

$$\alpha = \arccos\frac{\hat{\boldsymbol{n}}_{\text{ref}} \cdot \boldsymbol{B}_{\text{ref}}}{|\boldsymbol{B}_{\text{ref}}|} \tag{10}$$

The only manual control input to the ADACS is the pitch torquer current level. If the spacecraft is in passive mode (no active controlling of attitude), the current level can be a useful input to regulating the spacecraft's nutation and precession. Based on attitude and B-field data, the attitude estimation software computes the electrical current value that would be used in the active control mode of the ADACS for flight controller uplink if needed:

$$I_\theta = k_1 B_{\text{meas},x}\phi + k_2 B_{\text{meas},z}\phi + k_3 B_{\text{meas},z}\dot{\phi} \tag{11}$$

where the first term on the right-hand side provides precession control proportional to roll angle and roll-axis magnetic field. The next two terms provide nutation damping using the yaw magnetic field and a combination of roll angle and roll rate.

Implementation

The model was coded in an object-oriented language compatible with the popular laptop computer operating systems. A full graphical user interface (GUI) with pull-down menus and dialog boxes for data entry allowed smooth and easy operation.

Architecture

The program was written in an object-oriented manner with several libraries of unique routines. Figure 2 shows the basic structure of the various modules. Below the main program, there are three major groups of routines. First, on the left are the display control and dialog box routines. Second are the routines under DYNAMIC_IO, which control or generate input attitude data. Finally, on the right are the attitude synthesis routines including models, libraries, and estimation routines.

Data Flow

The spacecraft generates an ADACS data packet containing the measured nadir vector (roll and pitch) and the B-field as often as every 2 s. The GRAB_DATA routine extracts the data from the standard 9.6-kbps telemetry stream and alerts the EXECUTIVE that new data are available. The orbit propagator is updated, and the expected B-field is computed. The Jacobi algorithm (COMPUTE_K and JACOBI) is executed and generates the optimal quaternions, which are converted into Euler angles and body rates for display and plotting. All data are archived to facilitate postflight analysis.

GUI

For ease of use in a real-time operations environment, it was necessary to implement the software with a GUI. The commercial software development package used provided a simple way to generate a GUI with pull-down menus and dialog boxes for input. For output, the data were presented on a main window in numerical format and in a time-history graphics format for visual identification of attitude trends.

Table 1 describes the various controls and displays. Figure 3 shows the main display while an internal validation run is being performed. Reference roll, pitch, and yaw are +1, −3, and +4 deg. Three main menus are available and are used for program control. Numeric and graphical display areas present real-time information to the flight controller.

Verification and Validation

Verification and validation of the software took place in three venues. First, internal consistency of the attitude estimation algorithm was verified. A single attitude and orbit position was manually input, and the resulting output was checked for an estimate that made sense. The software also allowed the generation of a series of constant-input data points to check for correct subprogram initialization for multiple executions.

Second, a commercial orbit propagation program was used in conjunction with an attitude simulation program, supplied with the ADACS hardware, to provide a rigorous test of the estimator math models. An orbit state vector was given to the estimator as an initial condition, followed by a series of simulated attitude and rate points over a 10,000-s period in simulation time. No noise is added to these input values. This test is intended to show the functionality, not the robustness, of the software. The resulting attitude estimates and orbital positions were compared with the truth or reference from the attitude simulation program and the commercial orbit propagator. Figure 4 shows this comparison for a nominal initial attitude (0, 0, 0) deg with a +0.2-deg/s perturbation to yaw rate. Table 2 summarizes the mean three-sigma errors (estimated values minus truth values). In the fourth column, the angle errors are added in quadrature to known sensor measurement uncertainties. For roll and pitch, ±0.1-deg horizon sensor uncertainty is used. For yaw, ±2.0-deg magnetometer uncertainty is used. The magnetometer error is approximate, as the formal approach would be to propagate the vector B-field measurement uncertainty. In the last column, the model vs real-world uncertainties for the WMM95 magnetic field model (±0.71 deg) and for orbit propagation (±1.0 deg) are added in quadrature.

Table 1 Display screen descriptions

Item	Description
Menus	
Estimate	Start or stop estimation of attitude
Data source	Select source of data, e.g., disk file, communication ports, etc.
Setup	Set initial conditions for model and preferences for display
Numeric displays	
Date and time	Date and time of last telemetry received
Position	Geographic position and altitude of spacecraft
Measured attitude	Roll and pitch data from the horizon sensor
Estimated attitude	Best estimate of roll, pitch, and yaw
Estimated rates	Filtered x, y, and z (roll, pitch, and yaw) body rates
Orthogonality	B-field to nadir vector angle, indication of estimate accuracy
B-field error angle	Angle between expected and actual B-field vector
Pitch torquer command	Current level command to pitch torquer
Graphical displays	
Time history	Best estimate roll, pitch, and yaw as a function of time
Pitch axis	Pitch axis projection on LVLH x–z plane
Roll axis	Roll axis projection on LVLH y–z plane

Third, the telemetry interface was validated. A personal computer was used to generate a set of known, but random, values for the ADACS telemetry parameters and provide them in flight format over a serial connection to the estimator. The telemetry frame headers were recognized and the ADACS binary data decoded into engineering units. None of the estimation functions were exercised during this test. This test verified that all attitude control system data were correctly identified, calibrated, and entered into the estimator software data structures.

During mission operations training simulations known as joint integrated simulations (JISs), the flight crew and operations team come together in the NASA JSC's mission control center and Shuttle simulator to practice portions of the mission. Elaborate sets of broad computer simulations mimic the behavior of the Shuttle and its systems, as well as any payload or free flyer involved. All telemetry data are in flight format, and all relevant telemetry have flight-like values based on computer models. The JISs were to be the most rigorous and comprehensive tests of the attitude synthesis software prior to flight. However, the simplified geomagnetic field model used in the Shuttle mission simulator at JSC differed sufficiently from any of the models available for the estimation software to prevent verification. Because of the small amount of time remaining before

Table 2 Three-sigma attitude estimation uncertainties over 10^4 s

Axis	Angle, deg	Rate, deg/s	Angle, deg: Including sensors	Angle, deg: Including model
Roll	0.45	0.033	0.47	1.31
Pitch	0.35	0.005	0.38	1.28
Yaw	1.03	0.037	2.25	2.56

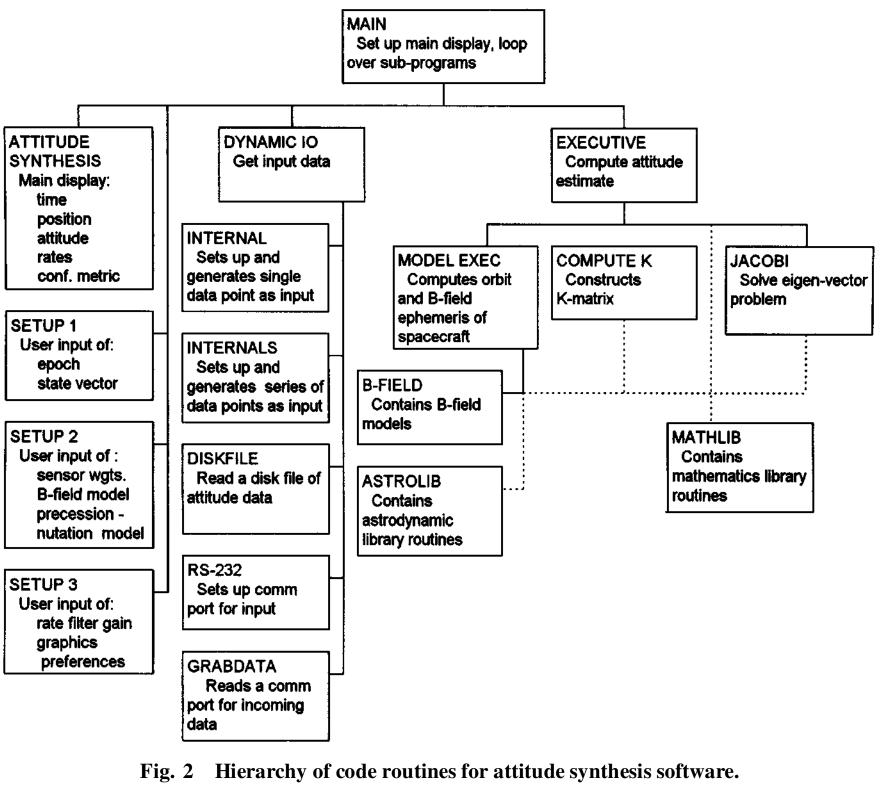

Fig. 2 Hierarchy of code routines for attitude synthesis software.

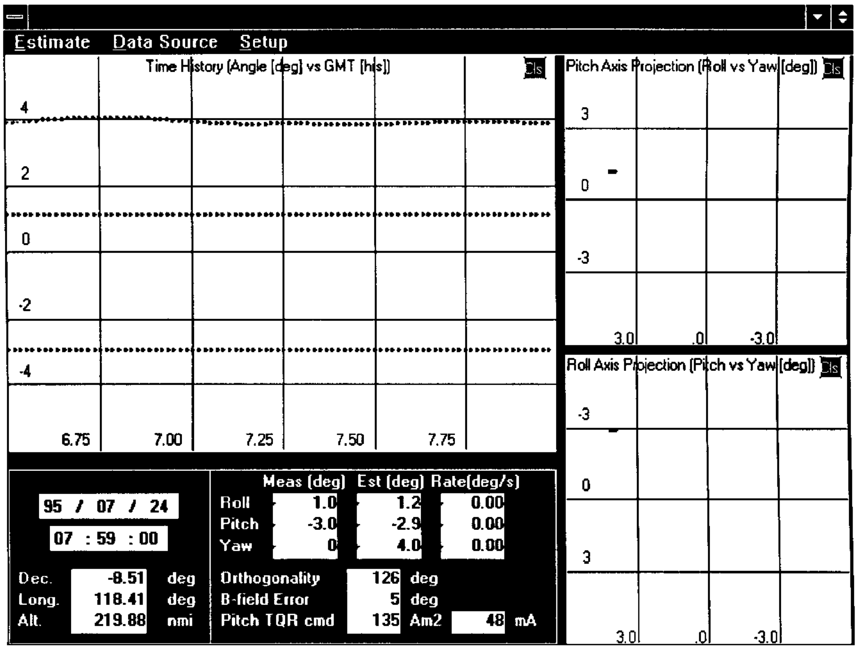

Fig. 3 Screen capture of attitude estimation program main display running internal validation.

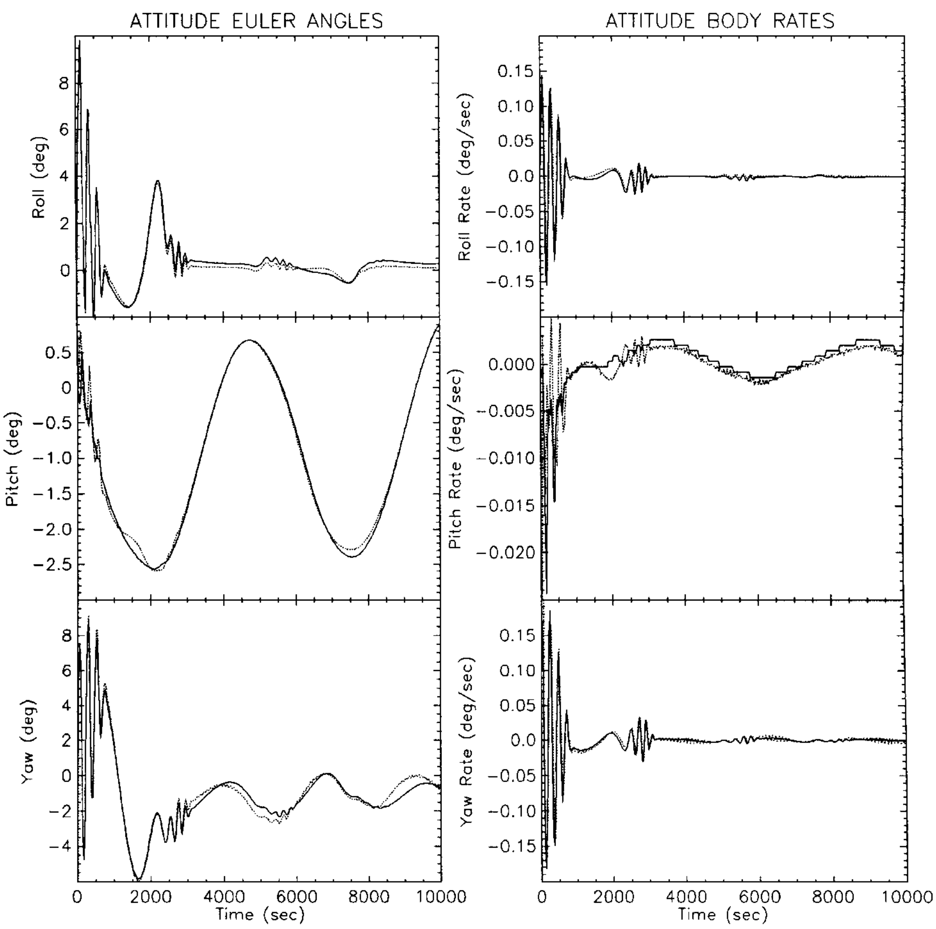

Fig. 4 Estimated angle and rate results (· · · · ·) compared to modeled angle and rate data (——).

flight, the first full end-to-end validation would come during WSF operations on STS-69.

Flight Operations Performance

During the STS-69 mission, the attitude estimation software performed well throughout most of the flight. It provided valuable insight into yaw angle and body rates, as well as backup attitude indications during periods of attitude anomalies. Reasonable and accurate attitude solutions were available about 90% of the time the telemetry stream was active. During the other 10% of the mission, occasional bad data points would cause display clutter and perturb the rate filters. These bad points were caused by incorrectly identifying other spacecraft data as having the ADACS packet header. The problem was corrected prior to STS-80. In addition, the program was adapted to postprocess archived roll, pitch, and B-field data for enhanced postflight analysis.

Archived data from STS-80 provide a good example of the effectiveness of the attitude estimation software. During the checkout period prior to release of the WSF, a number of Shuttle remote manipulator system (RMS) maneuvers are performed to verify the functionality of the attitude control system. These maneuvers are shown in Fig. 5a as recorded by the attitude estimation software. Because of pointing constraints associated with preparing the main spacecraft experiment for free flight, the checkout attitude (yaw, roll, pitch) is (0, 0, +10) rather than the free-flight attitude of (0, 0, 0). In addition, the Shuttle is in free-drift mode, and so gravity gradient and aerodynamic torques lead to slow oscillations about the (0, 0, +10) stable point. Foreknowledge of the Shuttle's absolute attitude was very uncertain as this was the first flight to use free drift extensively with a payload on the RMS. Thus, relative attitude maneuvers of the RMS, rather than absolute attitude checks, were used to verify the ADACS and the estimation software.

Table 3 shows the expected and observed changes in spacecraft attitude. The RMS roll maneuver is about the spacecraft x axis, which is pitched 10 deg. Thus, the RMS roll effectively acts on the spacecraft in a 3–2–1 Euler sequence rather than the attitude control system's 3–1–2 Euler sequence. This difference in sequences leads to observations of a positive RMS wrist roll as having a positive component in roll and a negative component in yaw. Thus, two channels of the estimation software were validated with only an RMS roll. Because the pitch angle is the final Euler rotation for the attitude control system, the RMS pitch maneuvers are observed in the pitch channel only. The agreement between the expected changes in attitude and those observed is very good. Using the expected uncertainties from Table 2, the yaw error was 1.2σ, roll error was 1.0σ, and pitch error was 0.1σ.

Figure 5b shows the WSF free-flyer attitude during the release and initial separation from the Shuttle. Prior to release, small drift rates due to the Shuttle's gravity-gradient oscillations are again evident. The increase in rates immediately following release, particularly in roll and yaw, indicate a probable tipoff from the RMS. After recovery from the tipoff, the thruster is activated. Yaw and pitch torques due to (allowable) thruster misalignment are clearly seen during the thrusting period. Following thrusting, the spacecraft ADACS slowly recovers its ideal attitude. It is clear that the estimation software provided valuable insight into the free flyer's attitude, as the yaw excursion was significant and would not have been observed otherwise.

Table 3 STS-80 on-orbit checkout results, deg

	WSF expected/observed		
RMS maneuver	$\Delta\psi$	$\Delta\phi$	$\Delta\theta$
$\Delta\phi = +15$	$-2.6/-2.8$	$+14.8/+14.2$	0.0/0.0
$\Delta\theta = +15$	0.0/0.0	0.0/0.0	$+15.0/+15.0$
$\Delta\theta = +5$	0.0/0.0	0.0/0.0	$+5.0/+5.1$
$\Delta\phi = +10$	$-1.7/-2.5$	$+9.8/+9.5$	0.0/0.0

Conclusions

An effective, accurate, and easily operable tool was developed to provide flight controllers a more complete understanding of the real-time attitude state of the WSF free flyer. Developed for a laptop computer, it allowed users to operate anywhere a data port was available. The accuracy of the resulting attitude estimates was significantly better than required by the main mission objectives and was quite sufficient for the critical phase of free-flyer separation from the Shuttle.

The kernel of the program has general applications to any overdetermined attitude problem and could quickly be adapted to include sun-sensor inputs. Star sensor inputs would take more time to accommodate because of the large database and search engines

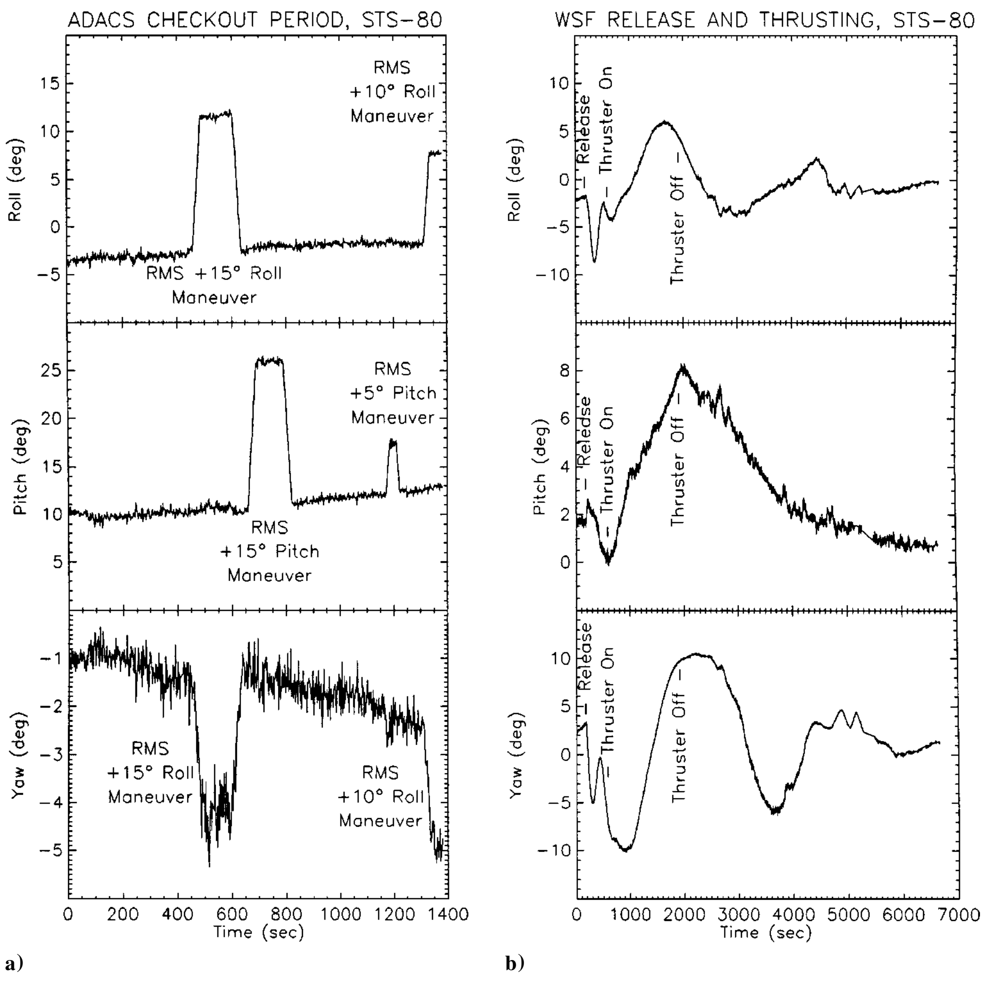

a) b)

Fig. 5 Performance of the ADACS and estimator during checkout and free flight.

required. In addition, with the computing power of today's space-rated computers, the attitude synthesis software could be ported to a low-cost embedded processor in an attitude control system for flight. Applying this optimal estimation approach has significant potential for reducing attitude sensing hardware costs.

Acknowledgments

The University of Houston's Space Vacuum Epitaxy Center provided the opportunity to develop this application for the Wake Shield Facility. The authors would like to thank Joseph Pineda and Arthur Rabeau for their assistance with the real-time telemetry handling, John Strozier for his help verifying the magnetic field models, and Jeremy Hang for rehosting the estimation software to new ground environment.

References

[1]Ignatiev, A., "The Wake Shield Facility and Space-Based Thin Film Science and Technology," *Earth and Space Review*, Vol. 4, No. 2, 1995, pp. 10–17.

[2]Selby, V., Tobey, B., Fox, S., Pal, P., and Hill, S., "An Attitude Control System for the Wake Shield Facility," *Guidance and Control 1993*, Vol. 81, Advances in the Astronautical Sciences, 1993, p. 456; also American Astronautical Society Paper 93-071, Feb. 1993.

[3]Bate, R. B., Mueller, D. D., and White, J. E., *Fundamentals of Astrodynamics*, Dover, New York, 1971, pp. 67–71.

[4]Meeus, J., *Astronomical Formulae for Calculators*, 4th ed., Willmann–Bell, Richmond, VA, 1988, pp. 63–67 and 93–96.

[5]Aeillo, J., "Spherical Harmonics," *Spacecraft Attitude Determination and Control*, edited by J. R. Wertz, Kluwer Academic, Norwell, MA, 1978, Appendix G, pp. 775–778.

[6]Plett, M., "Magnetic Field Models," *Spacecraft Attitude Determination and Control*, edited by J. R. Wertz, Kluwer Academic, Norwell, MA, 1978, Appendix H, pp. 779–786.

[7]Quinn, J. M., Coleman, R. J., Shiel, D. L., and Nigro, J. M., "The Joint US/UK 1995 Epoch World Magnetic Model," TR-314, Naval Oceanographic Office, NASA Stennis Space Center, MS, April 1995.

[8]Mortari, D., "ESOQ: A Closed-Form Solution to the Wahba Problem," *Journal of the Astronautical Sciences*, Vol. 45, No. 2, 1997, pp. 195–204.

[9]Lerner, G. M., "Three-Axis Attitude Determination," *Spacecraft Attitude Determination and Control*, edited by J. R. Wertz, Kluwer Academic, Norwell, MA, 1978, Sec. 12.2, pp. 420–428.

[10]Wahba, G., "A Least Squares Estimate of Satellite Attitude, Problem 65.1," *SIAM Review*, Vol. 8, July 1966, pp. 384–386.

[11]Markley, F. L., "Parameterization of the Attitude," *Spacecraft Attitude Determination and Control*, edited by J. R. Wertz, Kluwer Academic, Norwell, MA, 1978, Sec. 12.1, pp. 410–420.

F. H. Lutze Jr.
Associate Editor